Surface Plasmon Resonance Spectra of 2.8 ± 0.5 nm Diameter Copper Nanoparticles in Both Near and Far Fields

David B. Pedersen* and Shiliang Wang

Defence R&D Canada−Suffield, Suffield, Alberta, T1A 8K6, Canada

Received: June 29, 2007; In Final Form: September 12, 2007

Cu nanoparticles of 2.8 ± 0.5 nm diameter were synthesized in the gas phase using a sputtering−aggregation-type source. High-density films of nanoparticles were deposited onto NaCl substrates, and strong interparticle coupling was observed. In the near-field spectrum, the surface plasmon absorption was more intense than, and shifted 20 nm to longer wavelengths from, that observed in the far-field spectrum. These are the first near-field spectra of such small Cu nanoparticles, and the results agree well with theoretical predictions.

1. Introduction

Dominated by higher-order surface plasmon modes and severe damping of the dipolar surface plasmon resonance absorption, the absorption spectra of Cu nanoparticles appear very different from those of Ag and Au.[1] Unlike Ag, scattering contributes little to the overall extinction of Cu nanoparticles at wavelengths satisfying the dipolar surface plasmon resonance condition. Furthermore, the surface plasmon resonance is predicted to be a small feature in the extinction spectrum of copper nanoparticles (unlike Ag), and the interband electronic transitions, which are negligible in Ag nanoparticle spectra, are expected to be the dominant features. In some respects, copper shares these characteristics with gold, which is also predicted to have an extinction spectrum where scattering plays only a minor role.[1] One aspect unique to Cu, however (in comparison to Au and Ag), is that the appearance of its near-field spectrum is predicted to be totally different from that of its spectrum in the far field. The near-field extinction spectrum of small (22 nm) copper nanoparticles is predicted by electrostatic calculations to appear like that expected of a typical nanoparticle.[1] It has a prominent peak at visible wavelengths due to absorption by the surface plasmon of the nanoparticle. According to this theory, higher order surface plasmon modes are responsible for the near-field absorption, and the peak is shifted 22 nm from the peak position in the far-field extinction spectrum, accordingly. The near-field peak is also greatly enhanced in intensity relative to its far-field counterpart. By comparison, the surface plasmon peak appears as a relatively small bump in the far-field extinction spectrum. The enhancement and the 22 nm shift are predicted to be the primary differences between the far- and near-field spectra of copper nanoparticles. In this context, the near-field enhancement of the surface plasmon resonance absorption is due to growth of the multipolar absorption, which is inefficiently excited in the far field, to the red of the dipolar absorption. As the peaks are unresolved, however, the presence of the multipolar absorption *appears* to be a shift and growth of the dipolar absorption, which is incorrect. For Ag, on the other hand, the interband transitions appear at shorter wavelengths and do not damp the surface plasmon resonances as much as is the case for copper, so the dipolar absorption is typically dominant in both near- and far-field spectra.[1] Accordingly, the near- and far-field spectra look similar, unlike the copper case.

The amount of work done on copper nanoparticles is negligible compared to that done on Ag and Au. As most experiments are carried out in the far field, the relatively low extinction of the Cu nanoparticles is a disadvantage in typical applications involving surface plasmon resonance spectroscopy. Perhaps a greater disadvantage is that copper nanoparticles readily oxidize,[2] which makes oxygen-free environments prerequisite for working with copper. However, with the ever-increasing interest in applications exploiting nanoparticle near-field excitation,[3,4] one might expect copper nanoparticles to be utilized more extensively in the near future. One predicted advantage of copper is that near-field and far-field contributions to the extinction are easily distinguished. This contrasts Ag, for example, where the far-field and near-field spectra are predicted by electrostatic calculations to be effectively identical,[1] except for the enhanced multipolar absorptions that appear with near-field excitation.[5] The same is true for Au according to electrostatic theory.[1] A second advantage of copper, according to this theory, is that first-order surface plasmon excitation makes a relatively small contribution to the near-field spectrum.[1] Therefore, if one is relying on higher order surface plasmon excitations or utilizing techniques relying on strong near-field influences (e.g., surface-enhanced Raman scattering), spectra may be cleaner since there is little first-order or far-field background contribution to the overall signal. Much of this, however, is prefaced by the assumption that the theoretical predictions of the characteristics of near- and far-field spectra are correct, which, to our knowledge, has not been verified experimentally.

In a recent publication,[5] we demonstrated the utility of coupling internal reflection spectroscopy with the gas-phase deposition of high-density nanoparticle films as a way of studying near-field effects on the surface plasmon resonance spectroscopy of metallic nanoparticles. It was shown that, as the interparticle spacing decreased to values around 10 nm or so, near-field coupling between nanoparticles became pronounced. Spectroscopic features associated with near-field excitation, such as multipolar surface plasmon absorptions, were then observed. To distinguish far-field and near-field effects, we compared the transmission and internal reflection spectra of identical samples. The former showed no evidence of the

* Author to whom all correspondence should be addressed. E-mail: david.pedersen@drdc-rddc.gc.ca.

10.1021/jp075076x CCC: $37.00 Published 2007 by the American Chemical Society
Published on Web 11/02/2007

multipolar absorptions, while, in the latter, such features were prominent in the spectra. The evanescent wave present at the air−salt interface, where the internal reflection occurred, is well-known to provide the near field necessary to observe such effects.[3,6,7] Employing both small interparticle spacing and evanescent excitation, we were able to generate near fields strong enough that we could observe quadrupolar surface plasmon absorptions in 10 ± 5 nm diameter particles. Although internal reflection is not prerequisite for observing near-field effects, for the interparticle spacings and small particle sizes used, it was necessary to enhance the near field this way; otherwise, the field was too weak and multipolar absorptions were not observed. The observation of multipolar surface plasmon absorptions in such small nanoparticles is, to our knowledge, unprecedented. The groups of Chumanov and Cotton have also used high particle densities as a means of enhancing near-field effects on the surface plasmon spectra of larger (100 nm) Ag nanoparticles.[8,9] In that case, the near-field coupling was strong enough that no evanescent excitation was required to enhance the near-field effects. The appearance of the quadrupolar absorbance in the transmission (far-field) spectra obtained is evidence of the relatively strong near-field present in the larger particles. An interesting finding of their work is the effect of polarization on the near-field coupling. Because the nanoparticles were all in a plane, with s-polarization, near-field coupling of quadrupoles dominated the extinction spectrum. With p-polarization, such coupling was minimized, especially at larger angles of incidence, and more far-field-looking spectra were obtained. That is, the dipolar surface plasmon absorption prominent in far-field spectra was much larger than the quadrupolar one, which is known to be enhanced by the presence of the near field. One key advantage of our approach, compared to this work of Chumanov, is that our interparticle spacing can be varied systematically to very small values while being monitored spectroscopically. With increasing deposition time, the average nanoparticle spacing on a substrate decreases steadily from large to effectively zero. The ability to vary the spacing from 10−0 nm is particularly attractive as this is the region where near-field coupling between neighboring nanoparticles is most pronounced. This region is also beyond the current limits of lithography techniques, such as e-beam, which have a current resolution of ~10 nm. Our approach affords an opportunity to study the near-field spectra of high-density films of small nanoparticles with variable interparticle spacing beyond the resolution limit of other approaches.

Interparticle coupling interactions have been well studied in the context of nanoparticle dimers,[10−14] aggregates,[15,16] and films.[8,17−19] At relatively large distances, dipole coupling occurs readily. With decreasing interparticle separation, dipole coupling typically results in a shift of the surface plasmon resonance to longer wavelengths.[11,12,20−28] For ordered systems, shifts to shorter wavelengths may occur, depending on the polarization of the light with respect to the orientation of the nanoparticles. These shifts are typically much smaller in magnitude than the shift to longer wavelengths observed in non-ordered systems.[29,30] Much of this behavior can be explained in terms of electrodynamic interactions between particles.[31] When interparticle spacing is small (~10 nm or less), however, the electrostatic interactions between particles become important, and near-field coupling can occur. Under the influence of near fields associated with neighboring particles, higher order surface plasmon absorptions can occur in nanoparticles. As mentioned above, for the case of Cu, the resulting extinction spectra may then appear quite different from those observed under far-field conditions.

In the work presented in this paper, we utilized the gas-phase nanoparticle deposition technique to follow the coupling between 2.8 ± 0.5 nm diameter copper nanoparticles that occurred as the average interparticle spacing was systematically decreased. Using internal reflection spectroscopy, near-field coupling between the nanoparticles was observed. Unlike Ag,[5] for the Cu nanoparticles, extinction in the far field is weak. In the near field, extinction is much stronger. In fact, using the same light intensity and the same particle density, the observed extinction using near-field (s-polarized, internal reflection) excitation was 340 times that observed using far-field (nonpolarized, transmission) excitation. The spectra acquired agree well with the theoretical predictions for 22 nm diameter Cu nanoparticles.[1] To our knowledge, the near-field extinction spectrum of Cu nanoparticles has not been observed before. As the Cu, Ag, Au triad contains the simplest metals to treat theoretically, experimental spectra of such small Cu nanoparticles in both far and near fields are useful data for the continued development of theories dealing with light extinction by small metal nanoparticles and the effects of near- and far-field coupling interactions on such extinction.

2. Experimental Section

Copper nanoparticles were prepared in the gas phase by using a magnetron dc sputtering source described elsewhere.[5,32] Briefly, an oxygen-free high conductivity copper target (99.95%) with a 2 in. diameter and 3 mm thickness was attached to the sputter head, which acted as the cathode. The anode cap with a central hole 46 mm in diameter was placed 5 mm from the target. Ar, as the discharge gas, was introduced at a flow rate of 50 sccm (MKS 1179 gas flow controller) through a showerhead inlet directed at the anode cap and positioned immediately in front of the anode cap. The sputtered metal left the discharge and entered the aggregation zone where condensation and the formation of Cu nanoparticles occurred. A 10 sccm flow of He gas was introduced into the aggregation zone through a separate gas inlet. The nanoparticles then entered a secondary aggregation zone evacuated by a 500 L/s turbo pump (Varian V-550). Finally, the nanoparticles passed through an orifice into the deposition chamber where a pressure of $<10^{-4}$ Torr was maintained during deposition by a 300 L/s turbo pump (Varian TV-301).

The nanoparticles were deposited onto NaCl prisms (International Crystal Laboratories) positioned in the nanoparticle beam path and monitored by a UV−vis spectrometer in situ during the deposition process. Light from a halogen lamp was introduced into the deposition chamber through an optic fiber with a collimating lens attached to its end. For internal reflection mode experiments, the beam of light was incident through one side of the prism and internally reflected off of the interface where the nanoparticles were deposited. The reflected beam passed through the other side of the prism and left the deposition chamber through a quartz window. The reflected light was then collected by a second collimating lens and focused into another optic fiber that carried the light to the CCD array spectrometer (Ocean Optics, SD2000). Consecutive spectra were acquired every 2−3 s during deposition so that spectra of the nanoparticles could be obtained in real time, as they were being deposited. Alternatively, the deposition was monitored in situ in transmission mode, where light was passed directly through a NaCl plate (replacing the salt prism) at a normal angle. The NaCl plate with 2.5 mm thickness was made by filing down the back side of a salt prism and then water polishing. Polarized light was generated by placing a polarizer between the collimating lens of the incident light and the prism.

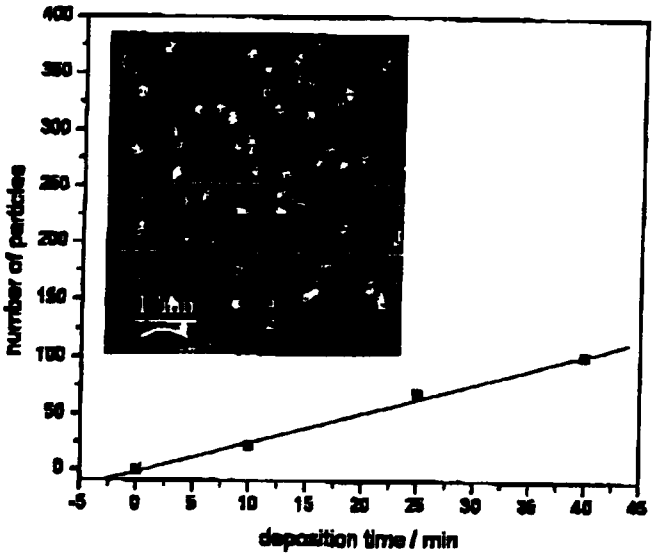

Figure 1. STM image of an HOPG substrate on which gas-phase Cu nanoparticles were deposited is shown in the inset. The image corresponds to a 25 min deposition. In order to acquire the STM images, these samples have been exposed to air, and the particles have been oxidized. The graph is a plot of the average number of particles in a 4733 nm^2 area, as determined from STM images, versus deposition time. Data values are shown as black squares. A solid line is shown as a guide to the eye.

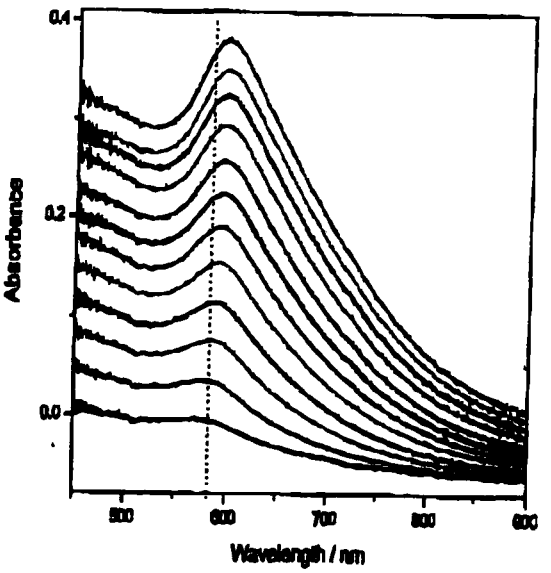

Figure 2. A series of transmission spectra acquired in situ during the deposition of Cu nanoparticles onto a NaCl plate. The lowest spectrum was acquired 1220 s after deposition was started, the second lowest 500 s later, and the rest every 400 s thereafter. The vertical dashed line marks the position of peak surface plasmon absorbance in the lowest particle density (1220 s deposition time) spectrum. For longer deposition times, there is an obvious shift of this band to longer wavelengths. Absorbance corresponds to $\log(I_0/I)$, where I is the intensity of light detected, and I_0 is the intensity of the light detected initially in the reference (i.e., before deposition began). Units are absorbance units.

The scanning tunneling microscope (STM) images of Cu nanoparticles deposited on graphite were obtained with the use of an easyScan E-STM (Nanosurf) operating in constant current mode. Fresh highly ordered pyrolytic graphite (HOPG) surfaces were obtained by peeling off the top layers with tape (3M-Scotch) before deposition. The HOPG substrate (SPI) was placed in the nanoparticle beam path at a similar position as the salt prism and salt plate. STM images were obtained immediately after the deposition was finished and the sample was exposed to air. All STM images were acquired in ambient air at a gap voltage of 0.03 V and a set-point current in the range of 0.2–1.0 nA.

3. Results

The correlation between Cu nanoparticle coverage and deposition time was examined utilizing STM and HOPG substrates. NaCl substrates used for spectroscopic measurements could not be examined directly, as they are nonconducting and incompatible with STM. A sample STM image is shown in Figure 1. Situated in front of the orifice connecting the nanoparticle source to the sample chamber, the HOPG substrate was exposed to the flux of nanoparticles for 25 min. The nanoparticles are clearly discernible as white circular features against the darker HOPG background. Higher deposition times yielded higher particle densities. A series of samples corresponding to 0, 10, 25, and 40 min deposition times were analyzed using STM imaging, and the particle density was determined. The results are plotted in Figure 1 as a plot of the number of particles versus deposition time. For deposition times less than 40 min, the nanoparticles were always well dispersed in submonolayer films, analogous to the results shown in the STM image in Figure 1. The possibility that the nanoparticles were partially oxidized via the presence of background O_2 in the deposition chamber and that this oxide layer prevented significant aggregation and coalescence from occurring was investigated. Variation in experimental parameters affecting oxidation, such as sample chamber pressure and the extent of oxidation of the Cu target, had no noticeable effect, and monodispersed films were always obtained. So it is more likely that the Cu particles were naked during deposition. It is clear that the amount of any oxide present on the particles was minimal. Venting the chamber to ambient air resulted in shifting of the spectra to longer wavelengths, consistent with formation of Cu@Cu-oxide core–shell nanoparticles.[33,34]

Monitoring the extinction spectra during nanoparticle deposition onto NaCl substrates in situ allowed the growth and shifting of surface plasmon resonances to be followed as the interparticle spacing steadily decreased with deposition time. A sample series of spectra is shown in Figure 2. These spectra are transmission spectra acquired using a NaCl plate. After 1220 s of deposition, the surface plasmon absorption could be observed. Note that longer deposition times are needed than for the STM measurements because of the relative insensitivity of the optical detection method. With increasing deposition time, the size of this peak increased steadily and shifted to longer wavelengths. Similar trends in the spectra were attained using internal reflection spectroscopy with s- and p-polarized light, with notable differences discussed below. A comparison of sample spectra acquired using transmission of nonpolarized, internal reflection of p-polarized, and internal reflection of s-polarized light is made in Figure 3. Light with p-polarization has the electric field vector parallel to the incident plane, as defined by the incident and internally reflected light rays. Because of the angle of reflection utilized, which must exceed the critical angle in order for internal reflection to occur, the largest component of the field vector of the p-polarized light was orientated perpendicular to the NaCl surface off of which the light was reflected. This places the field vector parallel to the evanescent field generated at the NaCl interface. The s-polarized light had the electric field vector entirely parallel to the plane in which the nanoparticles resided on the NaCl surface. As seen in Figure 3, the transmission and p-polarized reflection spectra appear very similar. The spectrum acquired via internal reflection of s-polarized light has a more

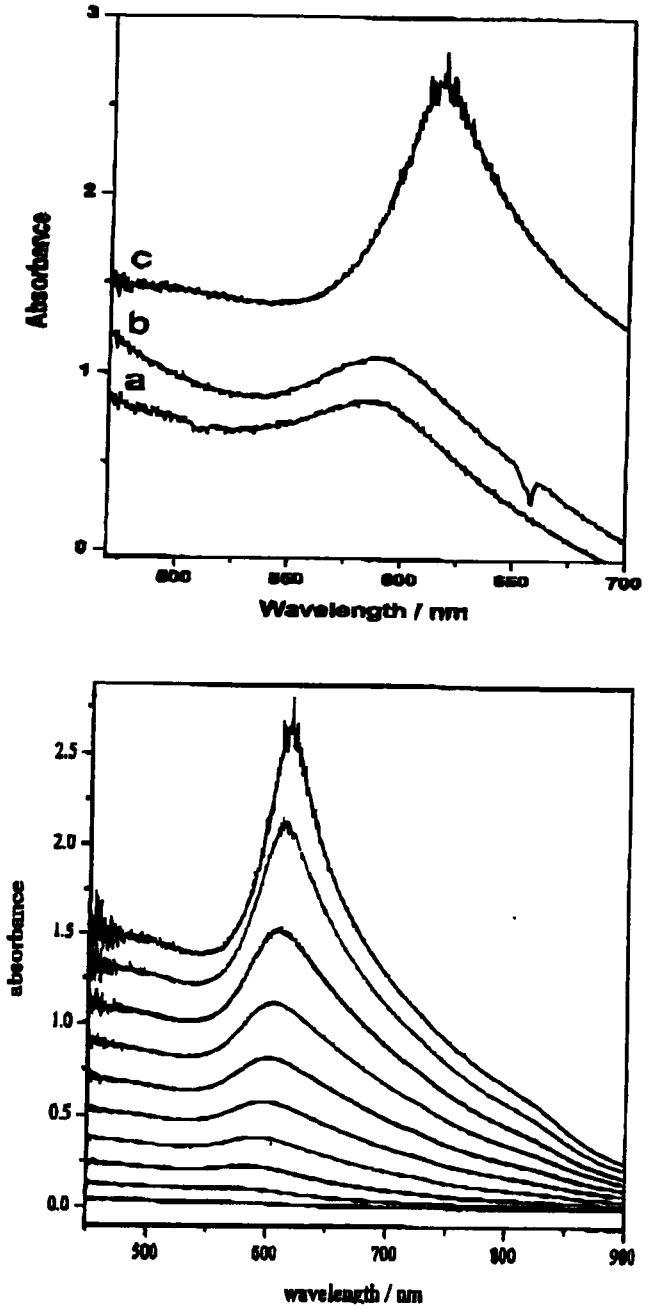

Figure 3. In the upper frame, spectra of Cu nanoparticles deposited onto NaCl were acquired in situ during deposition (a) using transmission of nonpolarized light, (b) using internal reflection of p-polarized light, and (c) using internal reflection of s-polarized light. The lower two spectra have been scaled by a factor of 10. Spectrum b has been offset vertically. The deposition time was 2100 ± 50 s for all samples. In the lower frame, data analogous to those in Figure 2 but for s-polarized light are shown. Absorbance corresponds to $\log(I_0/I)$, where I is the intensity of light detected, and I_0 is the intensity of the light detected initially in the reference (i.e., before deposition began). Units are absorbance units.

intense surface plasmon absorption that is significantly shifted from the peak position in the other spectra (also shown in Figure 3).

4. Discussion

The deposition of gas-phase Cu nanoparticles onto HOPG substrates resulted in submonolayer coverage of the substrates with monodispersed Cu nanoparticles. This fact is illustrated in Figure 1, where a sample STM image is shown. The nanoparticles appear clearly as white circular features against the darker HOPG background. As copper is known to oxidize readily,[2] and the STM images were acquired in air, it is most likely that the particles observed are in fact copper oxide, or at least Cu@Cu-oxide core–shell nanoparticles. However, the oxidation process is not expected to change the topography of the sample significantly outside of perhaps a small distortion of the shapes of individual particles. The fact that the particles are well dispersed in these images is almost conclusive evidence that the nanoparticles were initially deposited as well-dispersed, isolated nanoparticles. It is difficult to imagine a process whereby highly aggregated or even coalesced nanoparticles could be converted into well-dispersed collections of isolated nanoparticles, all nearly equal in size, via oxidation. Previous work has shown that monodispersed collections of nanoparticles are also produced on NaCl substrates.[5] Accordingly, although we have no way of using scanning microscopy to image Cu nanoparticle samples prior to exposure to air and the resulting oxidation, the evidence we do have, including the spectroscopy discussed below, strongly favors the assumption that the nanoparticles deposit onto NaCl as monodispersed films.

The spacing and size of the nanoparticles can be estimated from the STM images. Analysis of data such as that shown in Figure 1 indicates that the individual nanoparticles are 2.8 ± 0.5 nm in diameter, independent of deposition time. This estimate is likely high for two reasons. First, the well-known tip-distortion effect causes particles to appear slightly oval and slightly larger than they actually are. Second, the particles have been oxidized so the volume of the particles has likely increased to accommodate the intercalation of the oxygen into the particle. Spacing between nanoparticles is expected to vary with deposition time. Longer depositions produce higher particle densities in the submonolayer film that translate into smaller interparticle spacings. From STM images, the average interparticle spacing has been determined for samples with different deposition times. Good quality images could not be acquired for deposition times greater than 40 min, because the particle density was so high (approaching monolayer coverage) that the STM had little interaction with the underlying HOPG, and individual particles could not be distinguished from one another. The results attained for lower coverages are plotted in Figure 1. As seen, the number of particles per 4733 nm^2 area increased linearly with deposition time. There is also little evidence of aggregation and coalescence of the nanoparticles. Mathematically, because the particle flux (number of particles per unit area per unit time) is constant, it is straightforward to show that the interparticle spacing should be proportional to $t^{-1/2}$, where t is the deposition time, provided the process is statistical. That is, the particles deposit randomly on the surface in a submonolayer film. Ag nanoparticles were found to have behaved in such a way when deposited onto NaCl substrates.[5] The linearity of the plot in Figure 1, of number of particles per 4733 nm^2 against t, indicates that the deposition process is in fact a statistical one, and interparticle spacing is proportional to $t^{-1/2}$.

For randomly oriented nanoparticles, dipole coupling is well-known to manifest a shift of the surface plasmon resonance to longer wavelengths as interparticle spacing is decreased.[8,9,20,26,31] Appropriately, the series of transmission spectra in Figure 2 shows a gradual shifting of the surface plasmon resonance to longer wavelengths as the deposition time is increased, interparticle spacing decreased, and the extent of dipolar coupling increased. Initially, the peak of maximal surface plasmon resonance absorbance appears at 570 nm, slightly to the blue of the vertical bar. At this minimal particle density, interparticle coupling effects are minimal so the 570 nm value closely

approaches that of isolated Cu nanoparticles, albeit perturbed by the presence of the NaCl substrate. The 570 nm value agrees with other available data on Cu nanoparticles of comparable size, which have dipolar surface plasmon absorptions at 570 ± 10 nm.[33,35-37] The steady shift of this band to longer wavelengths is similar to that observed when Ag nanoparticles were deposited onto NaCl.[5] A major difference is that, for Cu nanoparticles, the shift is much smaller. For Ag, the dipolar surface plasmon absorption was observed to shift nearly 100 nm, even at submonolayer coverages. For Cu, the largest shift observed, as seen in Figure 2, was 15 nm. Clearly, the extent of dipolar coupling in Cu nanoparticles is much less than that for Ag.

For near-field coupling of adjacent nanoparticles in submonolayer films to be effective, the angle of incidence and the polarization of the light become important factors.[8] Typically, for internal reflection, one considers the near field strongest when using p-polarized light, as it is the out-of-plane (i.e., plane of the salt−air interface) component of the electric field associated with the incident light that generates the strongest evanescent field at the interface.[3] For the case of high-density nanoparticle films, however, near-field coupling between neighboring particles is more effective. As this type of coupling occurs in-plane, s-polarized light is more effective for observing near-field effects in these types of nanoparticle films.[8] A comparison of spectra attained using s-polarized reflection, p-polarized reflection, and nonpolarized transmission spectroscopy is shown in Figure 3. The transmission spectrum and the p-polarized spectrum are very similar in appearance. They both resemble the spectra acquired at low particle density, each having a surface plasmon resonance band at 570 nm as their prominent feature. The similarity of the two is not surprising, as both correspond to absorption under conditions of effectively far-field excitation. The spectrum acquired using internal reflection of s-polarized light, on the other hand, is different. The prominent feature in this spectrum occurs at 619 nm, significantly shifted from the 570 nm position of the dipolar surface plasmon resonance absorption in the other two spectra. Note that all three spectra correspond to 2100 s deposition times, so the nanoparticle density is the same for all three samples. Accordingly, the shift observed in the s-polarized spectrum cannot be attributed to more extensive dipolar coupling due to smaller interparticle separation as a result of a higher particle density. The shift is most likely that expected in the presence of strong near fields. Theoretically, the near-field spectrum of 22 nm diameter Cu nanoparticles (the literature result for particles closest in size to our 2.8 ± 0.5 nm diameter particles) is predicted to have a surface plasmon resonance peak red-shifted 22 nm from that observed in the far field.[1] Here, the multipolar absorption dominates, but, because of overlap of dipolar and multipolar absorptions, the two peaks are not resolved (as in the case of Ag),[5] but instead a shift in peak position toward the multipolar peak, positioned at longer wavelengths, occurs. The red shift predicted mirrors that observed experimentally for the 2.8 ± 0.5 nm diameter particles, as seen in the lower frame of Figure 3. This agreement between experiment and theory indicates that the s-polarized spectrum is dominated by near-field coupling between nanoparticles. Even more compelling evidence of the strong near-field nature of this spectrum is the large enhancement of the overall magnitude of the absorption. Note that, in the upper frame of Figure 3, the transmission and p-polarized spectra have been scaled by a factor of 10. At peak extinction, the amount of s-polarized light scattered and/or absorbed is 340 times that scattered and/or absorbed using p-polarized light or nonpolarized light in transmission. The large enhancement in extinction is a common characteristic of near-field excitation and is predicted to occur

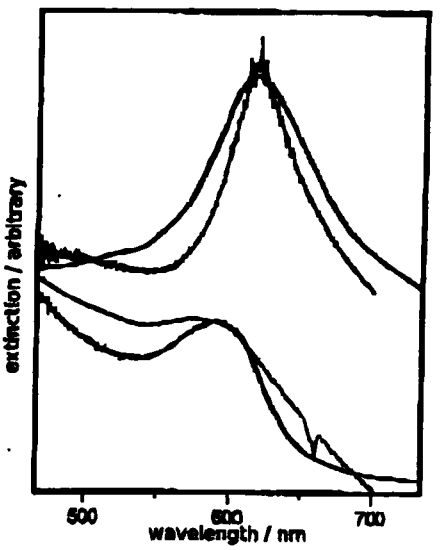

Figure 4. A comparison of the experimental reflection spectra acquired with s-polarized and p-polarized light with the theoretically predicted extinction spectra of 22 nm diameter Cu nanoparticles upon near-field and far-field excitation.[1] The theoretical spectra are black and have been shifted 29 nm to longer wavelengths so that the good relative agreement is seen without the distraction of the absolute (i.e., 29 nm) discrepancy. In the upper part of the figure the experimental s-polarized and theoretical near-field spectra are overlaid. In the lower part the experimental p-polarized and theoretical far-field spectra are overlaid. These latter two have both been scaled by a factor of 10.

for Ag, Au, and Cu nanoparticles of comparable size.[1,13,31] Spectra analogous to those shown in Figure 2, but acquired using s-polarized light in reflection mode (i.e., an attenuated total reflection spectroscopy configuration), initially appeared the same as those acquired using vertical polarization or transmission mode spectroscopy, as seen in the lower frame of Figure 3. Only after the particle density became higher, and the interparticle separation became smaller, did shifting and enhancement of the spectrum occur. As close proximity of the nanoparticles is required for near-field coupling to be effective, this behavior is consistent with the differences between the s-polarized spectrum and the others in Figure 3 being attributable to strong near-field interactions in the former but minimal in the latter.

The ability to tune the extent of near-field coupling between nanoparticles, by varying the polarization from s- to p-, affords an opportunity to acquire pseudo near-field and far-field spectra that can be compared with the theoretically predicted ones. Maximizing the extent of near-field coupling, by using relatively high particle densities and internal reflection spectroscopy and exploiting s-polarized light as a means of enhancing in-plane interactions between the Cu nanoparticles, yields a spectrum that is effectively a near-field spectrum. Avoiding these conditions allows spectra to be collected under far-field excitation conditions. In Figure 4 sample spectra of each type are shown, for our 2.8 ± 0.5 nm diameter particles, and compared with the theoretically predicted spectra for 22 nm diameter Cu nanoparticles. The theory predicts spectral peak positions at wavelengths 29 nm shorter than those observed experimentally, a factor compensated for in the figure by shifting the theoretical spectrum 29 nm to the red. There are a couple of possible reasons for the 29 nm discrepancy. First, the experimentally obtained spectra are not pure far-field or pure near-field; there is always some contribution from both. Second, the theoretical spectra are for an isolated particle in water, whereas the

experimental spectra correspond to high-density nanoparticle films where coupling interactions and a relatively high refractive index of the medium surrounding the nanoparticles, both of which may shift spectral features to the red, are present. The latter is most likely responsible for much of the difference observed. Outside of the 29 nm shift invoked, the overall agreement between theory and experiment is very good. Certainly, the relative peak positions of near-field versus far-field are well reproduced by theory. The relative peak heights are also correct. A remarkable characteristic of Cu nanoparticles of this size is that the near-field spectrum appears to be very different from the far-field spectrum. In this context, the spectra of the Cu nanoparticles are different from those of Ag, where near- and far-field spectra of particles of comparable size appear very similar.[1,10,13] For Cu, it is notable that, in experiments conducted under similar conditions, near-field excitation yielded more discernible peaks than observed with far-field excitation. Near-field excitation is therefore more suitable for applications dependent on the detection of surface plasmon resonances of Cu nanoparticles.

The good overall agreement between the experimental and theoretical results allows conclusions to be drawn regarding the nature of the near-field spectrum of small (<22 nm in diameter) copper nanoparticles. It is remarkable that the near-field spectrum of the high-density nanoparticle film resembles the theoretical spectrum of an isolated nanoparticle. Clearly, the near-field coupling between adjacent particles, which is prerequisite for the near-field spectrum to be observed in our experiments, does not distort the spectra significantly, and the spectrum acquired is effectively that of the individual non-coupled particles. It appears that the role of neighboring particles is solely to generate the near-field required; the presence of close neighbors does not alter the near-field spectroscopic properties of the nanoparticles, and no collective plasmon modes, as observed in the presence of far-field (dipolar) coupling,[8,12,20,22,26,28,31] result from the near-field interactions. This finding is somewhat in contrast to the expectations of Messinger et al.[1] that their results are not amenable to high-density arrangements (clusters) of nanoparticles. Clearly, they apply to the high-density monolayer types of films studied in our work. A second suggestion of Messinger et al., that it is not necessary to have peaks in near-field spectra appear at the same wavelengths as those in the far-field spectra, is fully supported by our experiments. As seen in Figure 4, the near-field and far-field spectra are quite different in appearance, and the peaks of maximal absorbance are shifted 22 nm from each other. According to theory, multipolar surface plasmon resonances and retardation effects give rise to additional peaks in the near-field spectra and manifest a shift of the surface plasmon resonance peak to longer wavelengths, as observed. This result is in sharp contrast to Ag, where far-field and near-field spectra, for particles in this size regime, are very similar in appearance. Cu nanoparticles are remarkable in this respect.

5. Summary and Conclusions

Spectra of 2.8 ± 0.5 nm diameter Cu nanoparticles have been attained under both far- and near-field excitation conditions. Decreasing the interparticle spacing, using evanescent excitation, and using s-polarized light were all found to be effective ways of enhancing the extent of near-field coupling between particles. When the near-field was maximized, spectra appeared different from those attained under far-field conditions. To our knowledge, these are the first experimental spectra of small Cu nanoparticles acquired using near-field excitation. These results demonstrate that Cu nanoparticles are different from Ag and Au analogues: the far- and near-field extinction spectra of Cu nanoparticles are quite different from each other, whereas the spectra of Ag and Au appear similar in both the far and near fields. Multipolar absorptions were the dominant features in the Cu spectra. Changing the magnitude of the near-field, however, changed only the intensity of the multipolar absorption bands. Their positions and shapes were unaffected. Despite the presence of multiple neighboring particles short distances away, the near-field features were identical to those expected in a spectrum of an isolated particle. Accordingly, spectra acquired under far- and near-field conditions agree very well with the theoretical spectra of isolated 22 nm diameter Cu nanoparticles. These experiments effectively confirm the theoretical predictions made by Messinger et al.[1] over 25 years ago.

Acknowledgment. The authors are grateful to J. Ho and R. K. Chang for their insight and helpfulness.

References and Notes

(1) Messinger, B. J.; von Raben, K. U.; Chang, R. K.; Barber, P. W. *Phys. Rev. B* **1981**, *24* (2), 649–657.
(2) Olynick, D. L.; Gibson, J. M.; Averback, R. S. *Appl. Phys. Lett.* **1996**, *68* (3), 343–345.
(3) Novotny, L.; Hecht, B. *Principles of Nano-Optics*; Cambridge University Press: Cambridge, U.K., 2006.
(4) Drezet, A.; Hohenau, A.; Krenn, J. R.; Brun, M.; Huant, S. *Micron* **2007**, *38* (4), 427–437.
(5) Pedersen, D. B.; Wang, S.; Paige, M. F.; Leontowich, A. F. G. *J. Phys. Chem. C* **2007**, *111* (15), 5592–5598.
(6) Krug, J. T. I.; Sanchez, E. J.; Xie, X. S. *J. Chem. Phys.* **2002**, *116* (24), 10895–10901.
(7) Wurtz, G. A.; Im, J. S.; Gray, S. K.; Wiederrecht, G. P. *J. Phys. Chem. B* **2003**, *107* (51), 14191–14198.
(8) Malynych, S.; Chumanov, G. *J. Am. Chem. Soc.* **2003**, *125* (10), 2896–2898.
(9) Chumanov, G.; Sokolov, K.; Cotton, T. *J. Phys. Chem.* **1996**, *100* (13), 5166–5168.
(10) Xiao, J. J.; Huang, J. P.; Yu, K. W. *Phys. Rev. B* **2005**, *71*, 045404-1–045404-8.
(11) Atay, T.; Song, J.-H.; Nurmikko, A. *Nano Lett.* **2004**, *4* (9), 1627–1631.
(12) Rechberger, W.; Hohenau, A.; Leitner, A.; Krenn, J. R.; Lamprecht, B.; Aussenegg, F. R. *Opt. Commun.* **2003**, *220*, 137–141.
(13) Jensen, T.; Kelly, L.; Lazarides, A.; Schatz, G. C. *J. Cluster Sci.* **1999**, *10* (2), 295–317.
(14) Su, K. H.; Wei, Q. H.; Zhang, X.; Mock, J. J.; Smith, D. R.; Schultz, S. *Nano Lett.* **2003**, *3*, 1087.
(15) Kelly, K. L.; Lazarides, A. A.; Schatz, G. C. *Comput. Sci. Eng.* **2001**, *3* (4), 67–73.
(16) Storhoff, J. J.; Lazarides, A. A.; Mucic, R. C.; Mirkin, C. A.; Letsinger, R. L.; Schatz, G. C. *J. Am. Chem. Soc.* **2000**, *122* (19), 4640–4650.
(17) Evanoff, D.; White, R.; Chumanov, G. *J. Phys. Chem. B* **2004**, *108* (5), 1522–1524.
(18) Al-Rawashdeh, N. A. F.; Sandrock, M. L.; Seugling, C. J.; Foss, C. A. J. *J. Phys. Chem. B* **1998**, *102*, 361–371.
(19) Liu, Z.; Wang, H.; Li, H.; Wang, X. *Appl. Phys. Lett.* **1998**, *72* (15), 1823–1825.
(20) Haynes, C. L.; van Duyne, R. P. *J. Phys. Chem. B* **2001**, *105*, 5599–5611.
(21) Wei, Q. H.; Su, K. H.; Durant, S.; Zhang, X. *Nano Lett.* **2004**, *4* (6), 1067–1071.
(22) Su, K. X.; Wei, Q. H.; Zhang, X.; Mock, J. J.; Smith, D. R.; Schultz, S. *Nano Lett.* **2003**, *3* (8), 1087–1090.
(23) Sandrock, M. L.; Foss, C. A. J. *J. Phys. Chem. B* **1999**, *103*, 11398–11406.
(24) Fort, E.; Ricolleau, C.; Sau-Pueyo, J. *Nano Lett.* **2003**, *3* (1), 65–67.
(25) Maier, S. A.; Brongersma, M. L.; Kik, P. G.; Atwater, H. A. *Phys. Rev. B* **2002**, *65*, 193408-1–193408-4.
(26) Bouhelier, A.; Bachelot, R.; Im, J.; Wiederrecht, G.; Lerondel, G.; Kostcheev, S.; Royer, P. *J. Phys. Chem. B* **2005**, *109* (8), 3195–3198.
(27) Haynes, C. L.; McFarland, A. D.; Zhao, L.; van Duyne, R. P.; Gunnarsson, L.; Prikulis, J.; Kasemo, B.; Kall, M. *J. Phys. Chem. B* **2003**, *107*, 7337–7342.
(28) Huang, W.; Qian, W.; El-Sayed, M. *J. Phys. Chem. B* **2005**, *109* (40), 18881–18888.

(29) Pinchuk, A.; Schatz, G. *Nanotechnology* **2005**, *16*, 2209−2217.
(30) Rechberger, W.; Hohenau, A.; Leitner, A.; Krenn, J. R.; Lamprecht, B.; Aussenegg, F. R. *Opt. Commun.* **2003**, *220* (1), 137−141.
(31) Zhao, L.; Kelly, K. L.; Schatz, G. C. *J. Phys. Chem. B* **2003**, *107*, 7343−7350.
(32) Pedersen, D. B.; Wang, S. *J. Phys. Chem. C* **2007**, *111*, 1261−1267.
(33) Zamkovets, A. D.; Kachan, S. M.; Ponyavina, A. N. *Phys. Chem. Solid State* **2003**, *4* (4), 627−631.
(34) Chatterjee, K.; Das, D.; Chakravorty, D. *J. Phys. D* **2005**, *38* (3), 451−455.
(35) Athawale, A. A.; Katre, P. P.; Majumdar, M. B. *J. Nanosci. Nanotechnol.* **2005**, *5* (6), 991−993.
(36) Jana, N. R.; Wang, Z. L.; Sau, T. K.; Pal, T. *Curr. Sci.* **2000**, *70* (9−10), 1367−1370.
(37) Johnson, R. C.; Li, J.; Hupp, J. T.; Schatz, G. *Chem. Phys. Lett.* **2002**, *356*, 534−540.